Enhanced Biophysical, Electrochemical & Computational Recognition of Cancer-Relevant G-Quadruplex DNA by Ferrocenyl Curcumin Schiff Base Motifs

Padma Sharma[a], Niki Sweta Jha[a*], Anupama Rai[a], Suresh Tiwari[b], Ranga Subramanium[b]

a: Department of Chemical Science & Technology, National Institute of Technology, Patna-800005, India

b: Department of Chemistry, India Institute of Technology, Patna-800005, India

Correspondence: Niki Sweta Jha, Associate Professor, Department of Chemical Science & Technology, National Institute of Technology Patna, Ashok Rajpath, Patna- 800005; E-mail: nikij@nitp.ac.in

Supporting Information

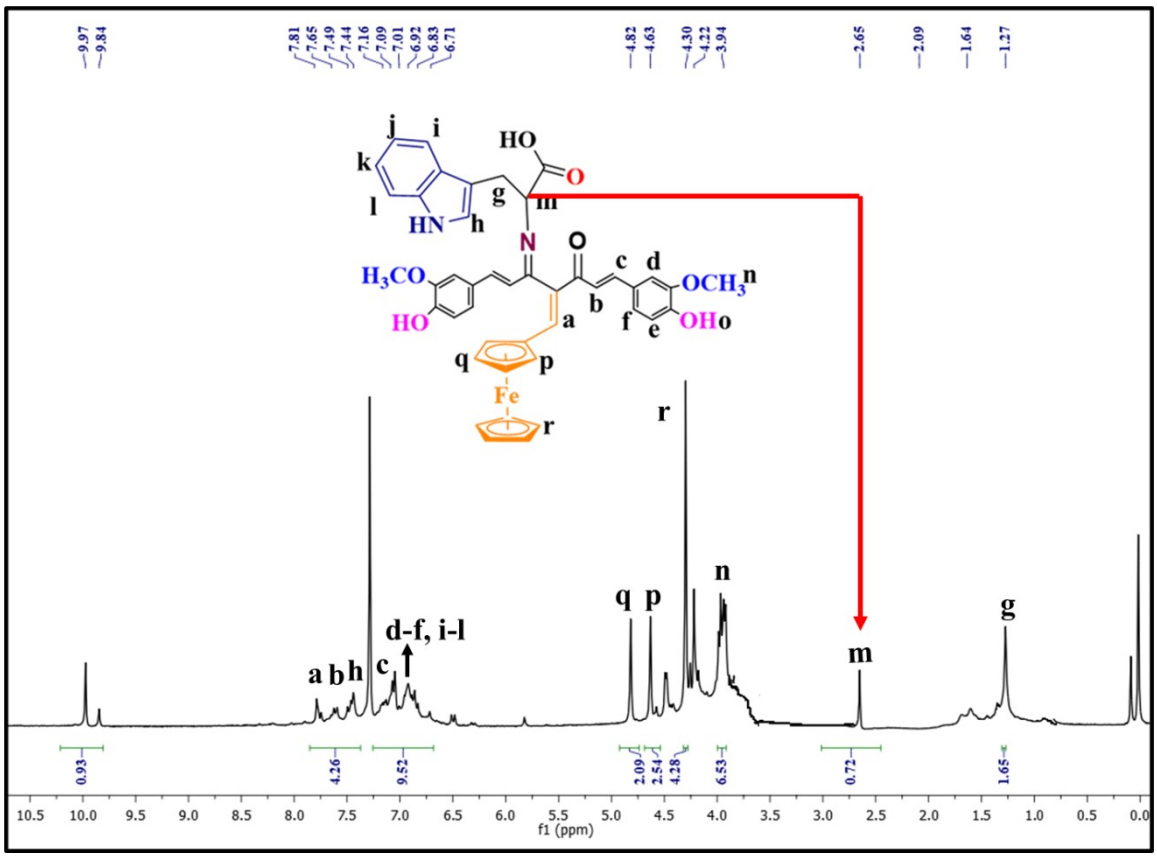

Figure S1. ^{1}H NMR spectra of synthesized compound Sb-Fc.

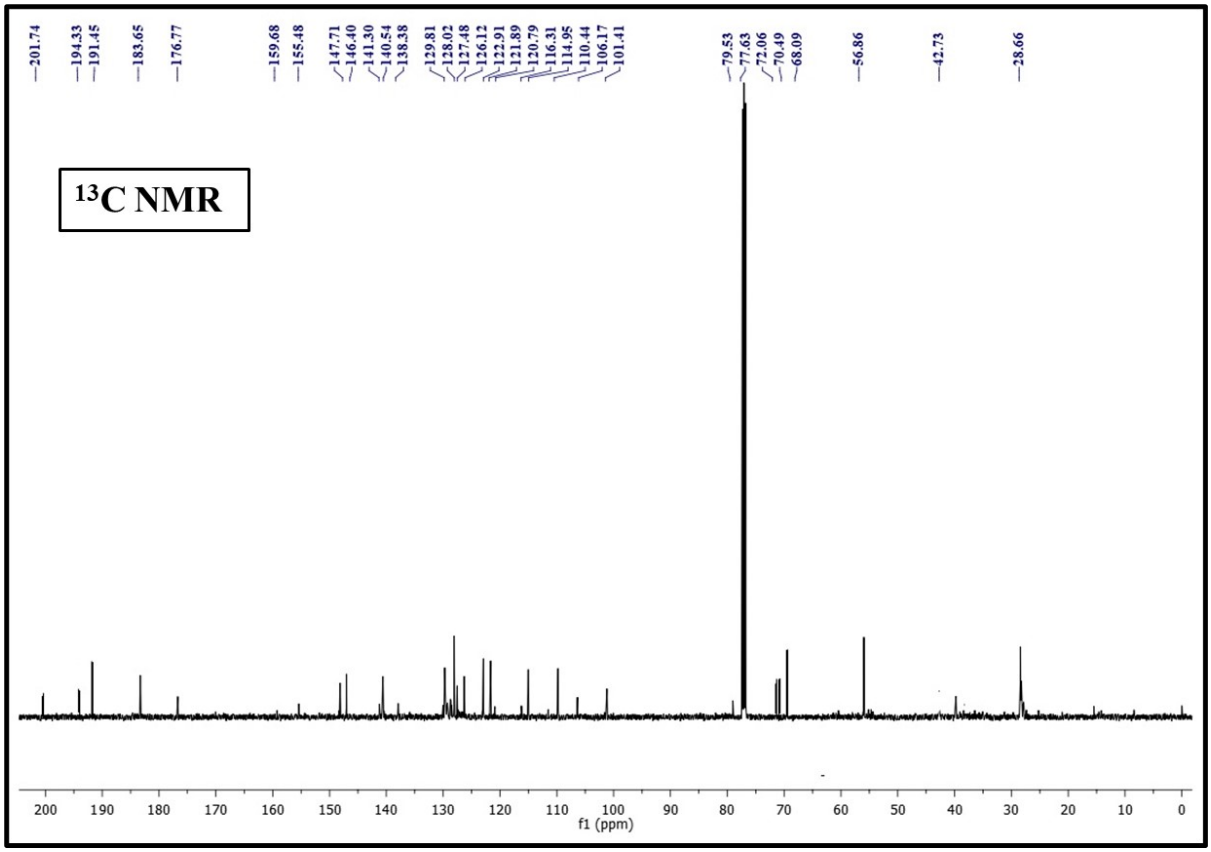

Figure S2. ^{13}C NMR of synthesized compound Sb-Fc.

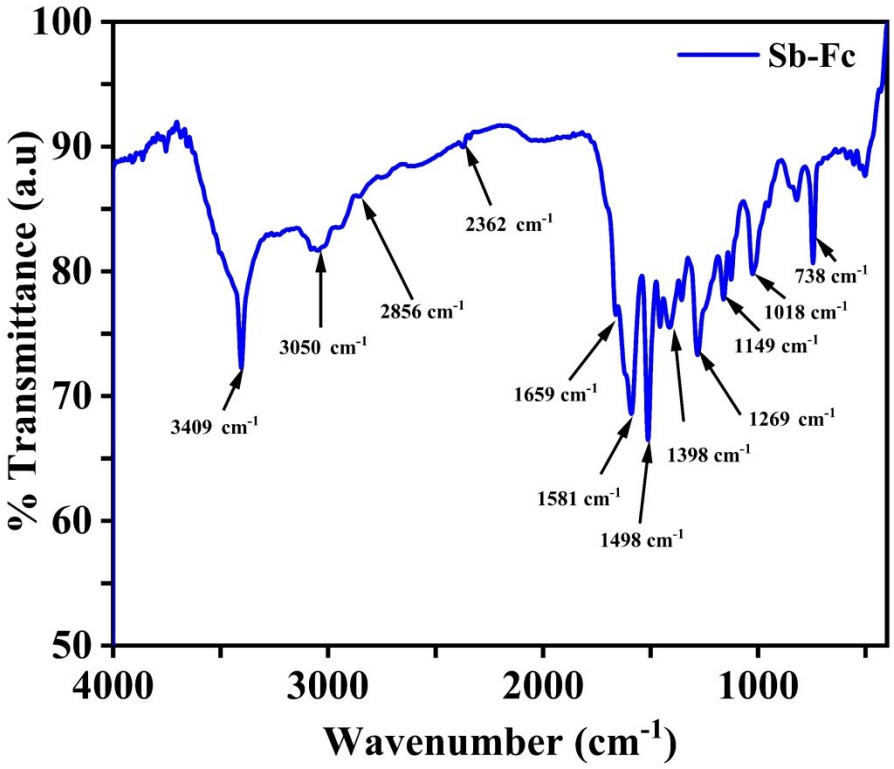

Figure S3. FT-IR spectra of synthesized compound Sb-Fc.

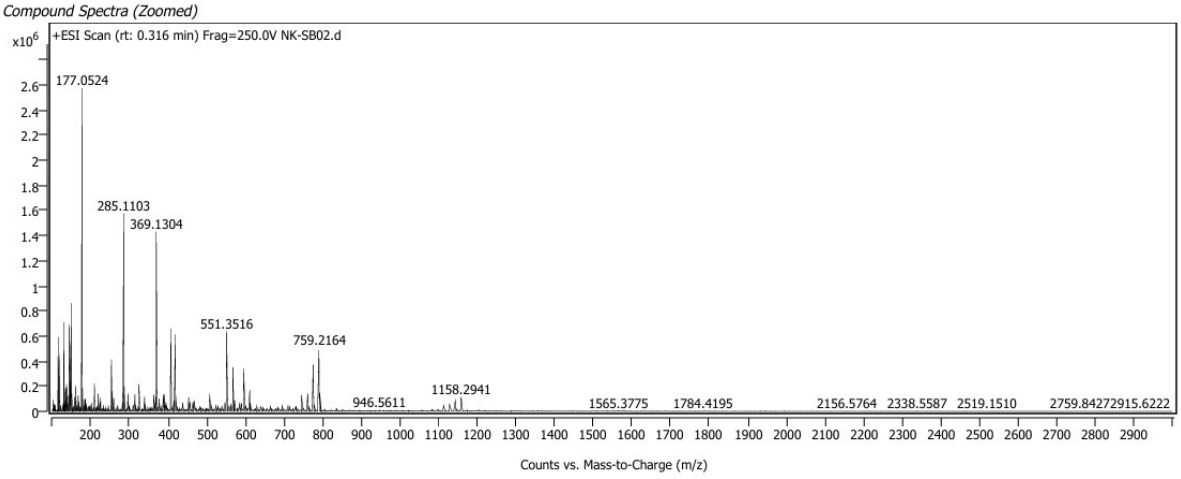

Figure S4. HR-MS of synthesized compound Sb-Fc.

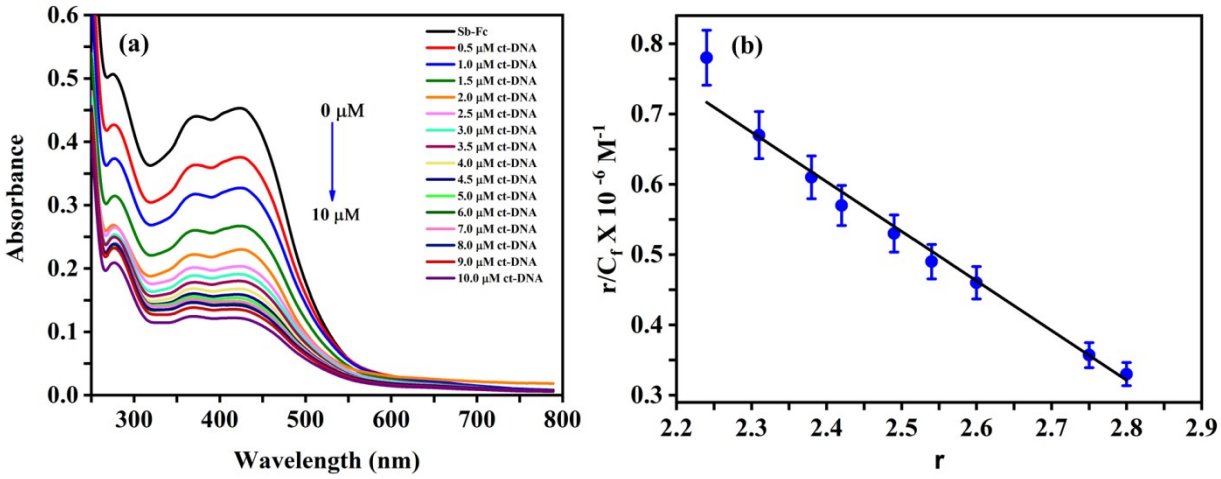

Figure S5. The **a**bsorption titration spectra of 10 µM (a) ct-DNA and (b) its Scatchard plot analysis of the interaction of Sb-Fc with 10 mM Tris buffer containing 0.01M KCl at pH 7.4.

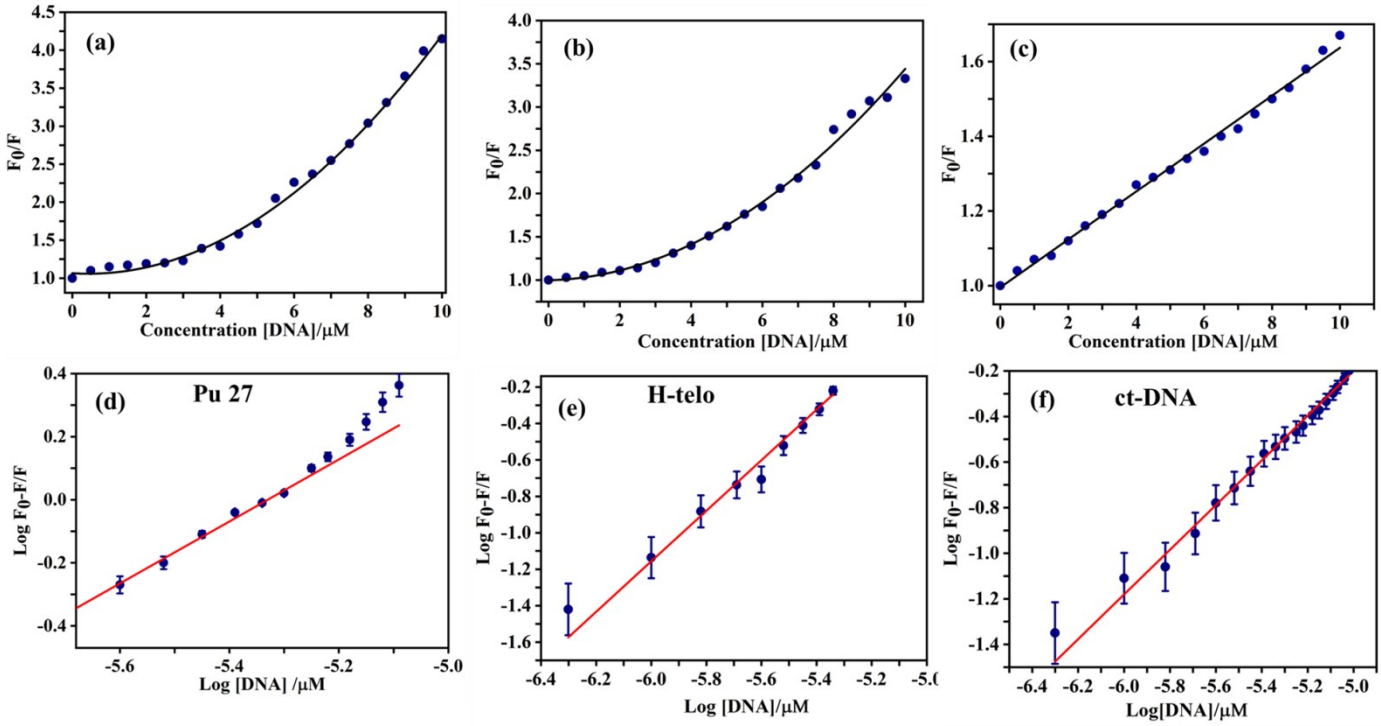

Figure S6: The variation of F_0/F vs DNA concentration and log (F_0-F/F) versus log [DNA] (a) Pu27, (b) H-telo, and (c) ct-DNA.

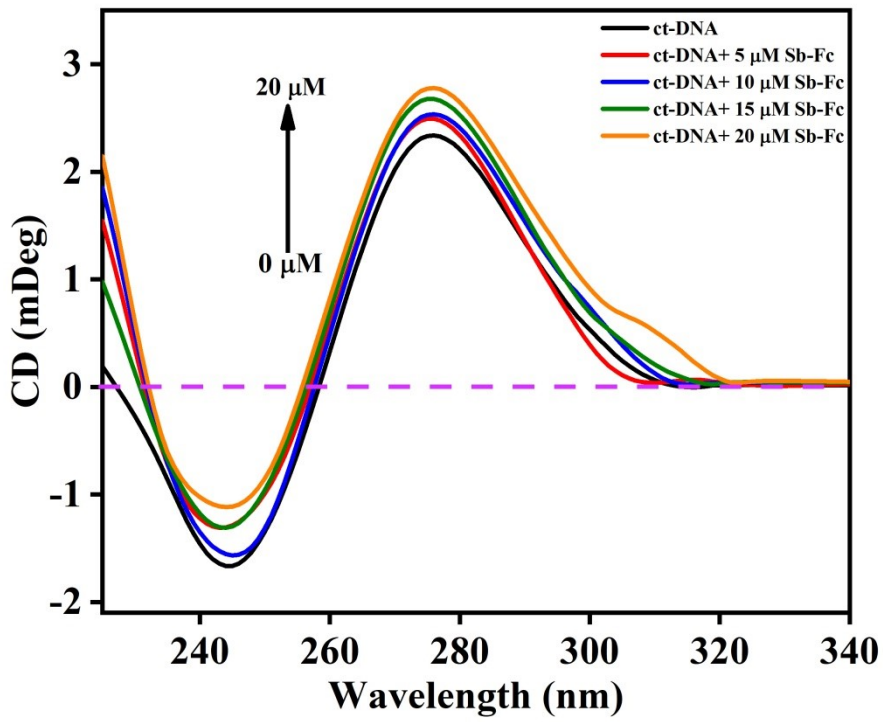

Figure S7: Circular Dichroism (CD) spectra of 10 µM ct-DNA by subsequential addition of 0-20 µM of synthesized schiff base (**Sb-Fc**) in 10 mM Tris buffer (pH 7.4), and 100 mM KCl.

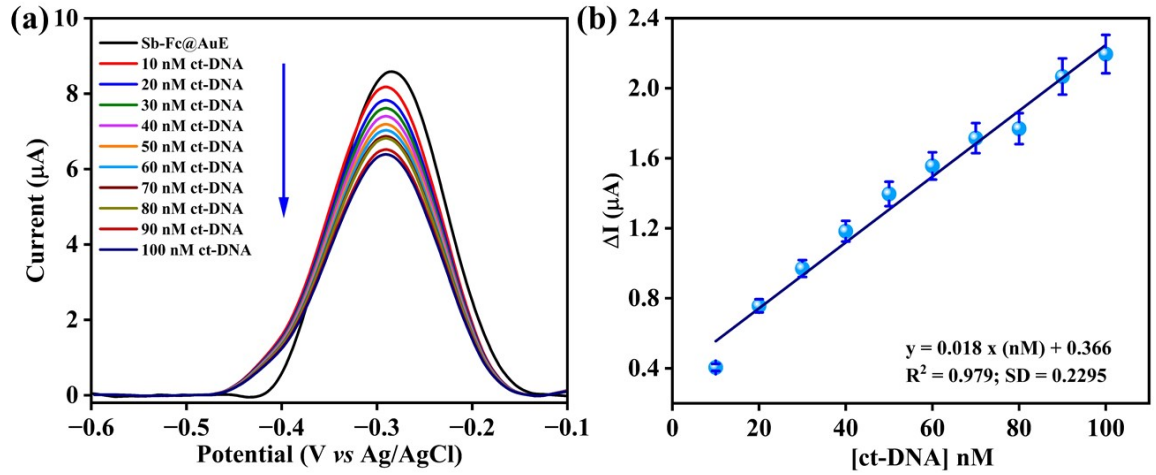

Figure S8: DPV curves obtained in 10 mM PBS buffer using Sb-Fc as probe for detection of ct-DNA, and calibration curve of DPV peak current decrease (I_0-I) with different ct-DNA.

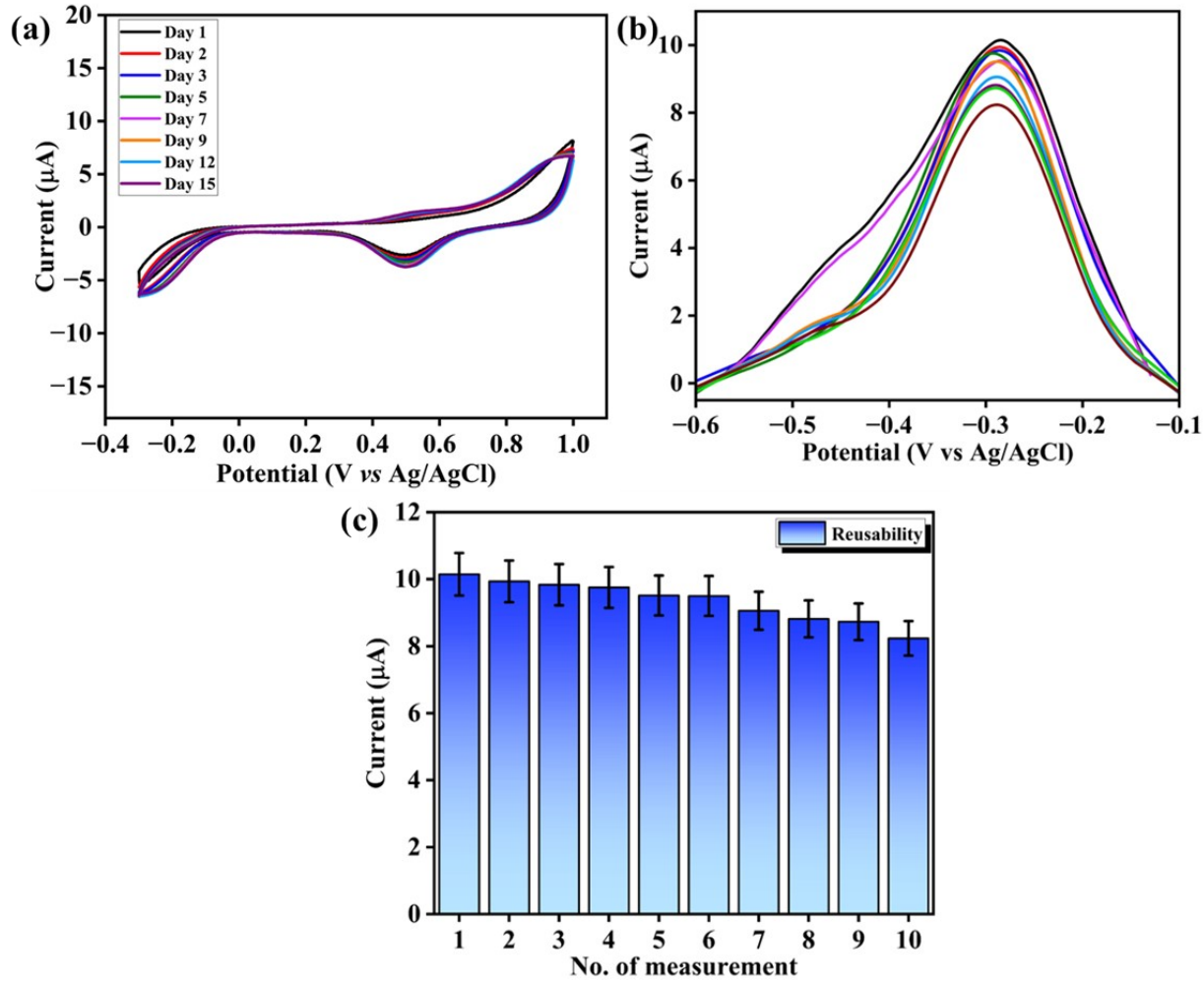

Figure S9: (a) Representative graph showing the stability of the Sb-Fc immobilized gold electrode over 15 days; (b) Differential pulse voltammetry (DPV) studies; and (c) representative bar graph illustrating the reusability of the Sb-Fc modified gold electrode for G-quadruplex sensing over 10 consecutive measurements.

Computational Studies

Curcumin-based ligands Coordinates:

C	-2.22027100	1.09101000	3.30854400
C	-1.21027200	0.54177100	2.51181600
C	-0.81170200	1.16220500	1.33258200
C	-1.41131300	2.36168500	0.91280000
C	-2.41702500	2.90832800	1.73002900
C	-2.82697900	2.29881300	2.91229400
H	-0.74193600	-0.39189900	2.81842600
H	-0.03234300	0.69938300	0.73579400
H	-2.90957500	3.83436200	1.44852900
C	-1.04289900	3.06995000	-0.31967800
H	-1.62077100	3.96814600	-0.52811900
C	-0.05945200	2.75207300	-1.17958700

H	0.60286900	1.90913300	-0.98318400
C	0.29865200	3.54597000	-2.39715300
C	1.54685600	4.36898200	-2.21378900
C	1.29373100	5.58817800	-1.38538600
C	2.42203700	6.32465200	-0.76904800
H	3.41771700	5.89831300	-0.81358400
C	3.14885100	8.35297100	0.55341700
C	4.51716900	8.05349900	0.67622900
C	2.67227300	9.55464200	1.12605400
C	5.38455400	8.91406500	1.34188600
H	4.91189900	7.13785400	0.24874600
C	3.53490600	10.41481200	1.78927700
H	1.61840400	9.79395800	1.03660200
C	4.90532700	10.09740100	1.90194900
O	-3.86002700	2.86032600	3.62054700
C	-3.54157400	3.32708600	4.93433700
H	-4.45333700	3.78799600	5.31980500
H	-3.24025200	2.50720500	5.59272300
H	-2.74413000	4.08074900	4.89866900
O	-2.65939400	0.49767800	4.45913000
H	-2.16428500	-0.32029100	4.59713200
C	2.97690300	-0.08999500	-1.68735100
H	1.90965100	-0.26370500	-1.69524100
C	3.66135800	0.93433500	-0.96510400
H	3.20233000	1.68331700	-0.33400200
C	5.05253400	0.83899100	-1.27292500
H	5.83180200	1.49036700	-0.90178700
C	3.94653100	-0.82006000	-2.44082100
H	3.73994300	-1.63856000	-3.11647700
C	5.22829400	-0.24684500	-2.18377700
H	6.16329100	-0.55685900	-2.62998900
C	2.54787400	2.00962900	-4.30509000
H	1.48158800	1.84373000	-4.30873800
C	3.25277400	3.05419300	-3.61000400
C	4.65194200	2.90269300	-3.92924200
H	5.44968500	3.52396100	-3.54337600
C	3.49885800	1.25232100	-5.04206600
H	3.27268500	0.38822500	-5.65158600
C	4.79877900	1.79813200	-4.81003400
H	5.73064600	1.41975100	-5.20720900
Fe	3.95812200	1.17751700	-3.00933000
O	0.12682000	5.96349700	-1.21747800
N	-0.33560500	3.61308000	-3.50373900
C	-1.53101400	1.89901000	-4.75630900
O	-0.51746000	1.38114700	-5.17244600
O	-2.75691400	1.50241700	-5.18281100
H	-2.59147400	0.79303300	-5.82635800
C	-1.83480300	6.04068500	-5.37486400
C	-2.02529700	6.45074300	-6.72289500
C	-1.44983900	7.61607500	-7.24145400

C	-0.67201600	8.38209800	-6.38093300
C	-0.47175900	7.99533400	-5.03930400
C	-1.04021100	6.83480000	-4.52877100
C	-2.57845200	4.81560400	-5.19125400
H	-1.60500300	7.91177600	-8.27573100
H	-0.20966900	9.29360200	-6.74961300
H	0.14558900	8.61560900	-4.39556500
H	-0.86371500	6.53930600	-3.49916800
H	-3.15297800	5.53671800	-8.28049100
C	-3.17197600	4.53957800	-6.39918300
H	-3.81540800	3.71516100	-6.67160700
N	-2.84133300	5.51280300	-7.32401200
C	-2.72606000	4.01218300	-3.92971200
H	-2.73223500	4.68233100	-3.06337400
H	-3.68580200	3.48710100	-3.93324100
C	-1.62009400	2.95206100	-3.65980700
H	-1.92588400	2.38863700	-2.76256000
C	2.19255200	7.49281200	-0.13216800
H	1.15721700	7.83163400	-0.13301100
C	2.77336800	4.10662100	-2.72766800
H	3.55937100	4.81303500	-2.47089900
O	3.19811400	11.60618800	2.38408500
C	1.84275700	12.02830900	2.32179100
H	1.79760800	12.98503400	2.84373200
H	1.51552300	12.16399500	1.28374500
H	1.17906000	11.31066300	2.81940300
O	5.74930900	10.93812200	2.55103500
H	5.22060800	11.69168100	2.85775000
H	6.44104200	8.68736200	1.43951200

Table S1. Theoretically Calculated Gas-Phase Vibrational Frequencies of the Sb-Fc Compound at the B3LYP/6-31G(d,p)/LANL2DZ level of theory with scaling factor (0.9608).

Frequencies	**IR intensity**
5.47	0.0549
6.45	0.5165
10.25	0.8173
11.23	0.0351
12.86	0.1221
15.63	0.2148
18.63	0.7257
23.44	0.2472
30.49	0.2165
30.74	0.1188
34.86	0.0811
44.87	0.2166
48.38	0.1955
51.57	0.5305
60.42	1.2746

63.38	1.212
68.24	4.9793
73.45	2.445
78.2	1.2782
79.46	2.5013
83.73	1.9254
97.33	2.822
107.2	2.1561
116.06	0.157
127.88	3.7717
130.32	0.8726
141.54	0.877
151.96	2.1314
157.76	0.153
167.26	1.769
167.71	0.8728
170.91	0.2389
180.57	2.9539
210.13	3.0636
215.43	8.0025
218.25	1.553
218.71	1.3091
221.9	1.2615
228.79	1.2026
241.4	6.2097
260.84	0.5447
272.21	1.2161
279	0.9109
281.23	1.2017
288.64	7.9169
290.42	15.36
315.77	11.66
324.67	4.5892
325.94	25.3012
332.15	12.2005
333.6	68.5094
351.83	4.1119
356	16.1094
363.79	13.9108
368.15	18.7902
371.83	10.5697
387.73	5.4028
410	44.3694
422.89	1.5225
425.93	5.6691
429.75	18.2033
433.97	32.072
440.07	20.8425

442.4	9.375
443.74	12.5743
450.13	2.3905
473.03	2.2088
473.95	91.8188
480.37	30.2878
491.14	28.1538
519.14	4.362
527.42	11.3204
538.77	3.9093
541.05	12.543
542.61	12.448
548.93	13.0348
549.34	1.1494
552.09	0.0545
560.01	9.7451
562.72	1.3109
570.33	7.2566
576.02	34.9612
579.92	21.2038
587.32	5.3292
603.24	7.5969
615.92	19.8289
622.1	24.385
626.3	3.137
649.64	62.056
681.75	1.2666
687.65	13.0791
693.86	28.91
702.88	10.4467
708.59	15.7737
717.16	24.4218
726.16	10.7763
727.99	56.8865
732.36	8.3962
742.07	6.539
751.58	3.9285
765.39	5.5571
774.61	21.4235
776.7	4.8422
779	1.1185
784.02	16.5724
786.78	2.0959
789.81	51.5599
797.33	15.6345
802.72	7.8208
805.51	7.2683
808.88	7.0306

811.89	0.606
814.62	10.8583
818.34	4.6751
823.99	7.062
826.13	10.0034
827.02	12.1977
831.85	23.9652
843.17	2.7128
845.98	0.1911
850.22	0.4504
852.29	0.6138
852.72	3.767
870.41	3.9725
881.05	15.3675
884.82	9.3381
888.37	3.8825
891.5	0.4048
899.89	2.636
904.67	1.6251
908.48	9.8007
911.19	14.61
916.33	13.8007
922.2	11.0917
941.51	24.3997
945.53	3.906
959.77	48.4684
965.3	9.7588
986.46	7.8331
988.45	4.8823
991.7	17.2447
1001.36	7.7975
1014.34	65.4954
1021.85	8.1611
1026.7	46.8753
1030.5	1.6658
1036.36	35.8566
1037.15	7.8401
1037.83	49.2477
1047.08	45.842
1047.87	64.6836
1068.36	32.2953
1084.85	90.1829
1089.88	10.7493
1095.14	106.7168
1105.69	33.1223
1109.33	13.4078
1124.36	250.7042
1132.01	0.5544

1132.32	4.1135
1136.08	49.8172
1145.8	91.4104
1147.61	30.6594
1153.04	136.2169
1155.63	239.3813
1169.92	11.0828
1173.06	38.0008
1186.79	2.8413
1187.6	191.5634
1193.38	6.8344
1205.58	20.5026
1217.27	86.2044
1224.41	268.6986
1225.55	70.2183
1237.12	17.8644
1241.69	0.1759
1243.77	2.8723
1249.15	60.618
1263.58	75.736
1264.13	354.1434
1272.84	2.0663
1277.28	9.1425
1278.21	89.6128
1281.07	337.6019
1294.61	29.7766
1297.72	45.8875
1300.36	11.1563
1318.33	29.2317
1320.84	20.9969
1326.3	75.1143
1328.59	22.5984
1334.54	32.6508
1337.01	5.1121
1341.87	4.8292
1358.08	15.0524
1361.7	12.6631
1368.83	34.8003
1376.42	26.9283
1394.58	25.7623
1396.76	22.5987
1401.87	18.5184
1405.65	1.9462
1406.02	1.0453
1412.29	13.364
1429.73	8.8318
1432.81	7.1278
1437.21	37.7522

1437.57	22.1205
1439.3	5.1953
1441.45	6.5889
1442.8	26.6361
1458.28	56.9624
1464.01	10.2848
1474.51	4.8139
1499.08	172.6245
1502.09	435.1771
1537.04	20.328
1562.64	614.6756
1566.15	18.6834
1572.37	44.5925
1583.73	63.9792
1594.05	40.5478
1598	26.0368
1604	239.7692
1608.21	5.5327
1627.7	34.6815
1640.99	160.6936
1652.07	150.4042
1761.05	271.3198
2865.35	24.9532
2905.42	41.6292
2906.22	69.4794
2939.71	21.0089
2967.85	31.2009
2984.3	39.8776
2985.06	14.6574
3021.58	24.5953
3023.7	9.0566
3029.97	27.1139
3035.75	22.3041
3038.32	1.2435
3041.18	12.3418
3046.78	0.2334
3046.95	7.5309
3056.97	30.3458
3069.79	30.9457
3073.23	9.3009
3074.04	4.3497
3075.56	5.6634
3080.78	5.1066
3083.9	1.8044
3086.08	8.56
3090.55	9.9695
3111.17	1.4481
3114.88	0.1904

3116.55	0.2719
3122.26	6.7312
3128.78	11.7432
3130.02	8.1784
3134.43	7.5194
3137.38	1.2767
3140.46	1.6474
3159.08	60.8386
3544.88	73.1174
3603.29	63.0041
3611.96	168.7472
3670.44	69.3611

S1. FMO Analysis:

A molecule's chemical activity is determined by its frontier molecular orbitals (FMO), especially its lowest unoccupied molecular orbital (LUMO) and its highest occupied molecular orbital (HOMO). These orbitals control a molecule's interactions with other species.[1] One crucial measurement of chemical reactivity is the energy gap between the HOMO and LUMO; a smaller gap indicates stronger reactivity, greater polarizability, and lower kinetic stability-all of which are traits frequently found in soft molecules.[2] This work used the B3LYP/6-31G(d,p) and LANL2DZ levels of theory to compute the HOMO-LUMO energy gap of ligands UNK0. The frontier molecular orbital (FMO) analysis of the UNK0 ligand reveals that the highest occupied molecular orbital (HOMO) is predominantly spread across the tryptophan unit, underscoring its electron-donating characteristics. In contrast, the lowest unoccupied molecular orbital (LUMO) is chiefly situated on one side of the curcumin framework, with a slight contribution from the ferrocene moiety, indicating a charge transfer towards the acceptor region. This clear spatial division of frontier orbitals not only supports the behavior of intramolecular charge transfer but also confirms an effective donor-acceptor electrical configuration. The narrow FMO energy gap of 0.1120 eV suggests improved electron delocalization and molecular polarizability, which could enhance π–π stacking and electrostatic interactions with nucleic acid base pairs, potentially resulting in more stable ligand-DNA interactions.

Additionally, TD-DFT calculations were performed to explore the electronic absorption properties of the Sb-Fc (UNK0) ligand and to compare them with the experimental UV-Vis spectrum. The simulated spectrum {**Figure S10(b)**} reveals a strong absorption band in the visible range, primarily resulting from a HOMO → LUMO transition with significant π–π*

and intramolecular charge-transfer (ICT) characteristics, aligning with the donor–acceptor electronic structure identified by FMO analysis. Experimentally, the Sb-Fc (UNK0) ligand shows a shoulder band at 365 nm and a prominent absorption peak at 425 nm, attributed to π–π* transitions within the conjugated curcumin framework, along with contributions from aromatic and azomethine chromophores. The red shift observed in the calculated spectrum compared to the experimental one is mainly due to the gas-phase approximation used in TD-DFT calculations, which does not account for solvent and environmental effects. Nonetheless, the computed results capture the overall spectral features and confirm effective electronic delocalization and charge-transfer behaviour within the ligand framework.

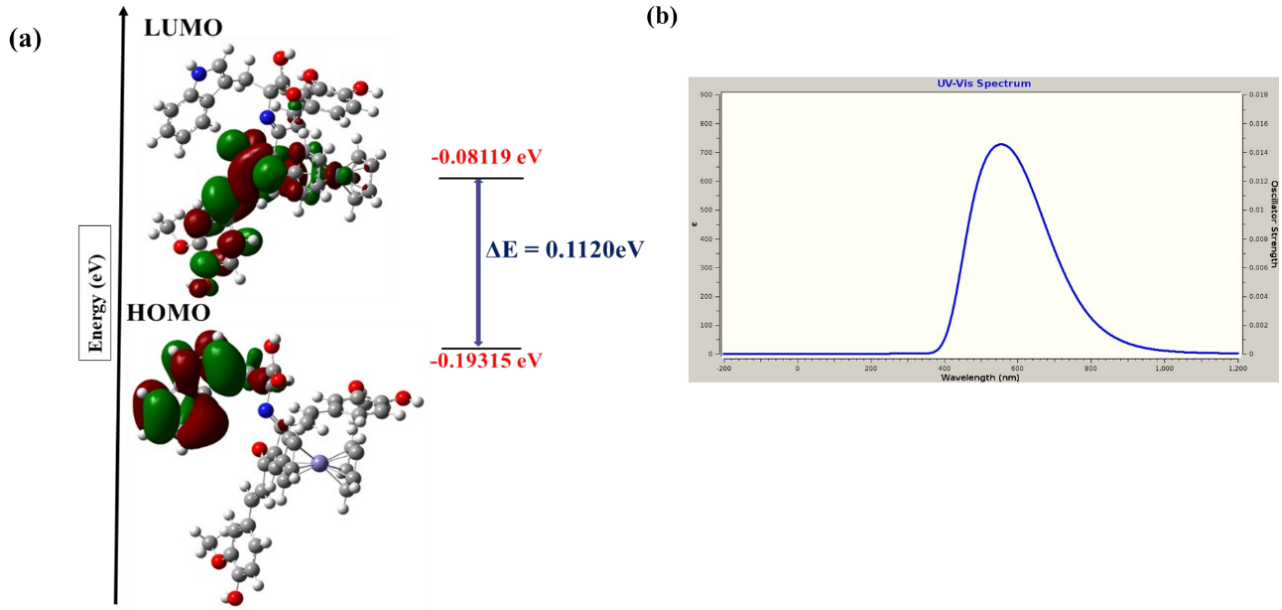

Figure S10. (a) FMO and (b) TD-DFT of UNK0 were obtained from the B3LYP/6-31G(d,p) and LANL2DZ level of theory.

S2. Molecular Electrostatic Potential (MEP) Analysis:

A three-dimensional molecular electrostatic potential (MEP) map graphically represents the charge distribution within a molecule. By highlighting areas of positive and negative charge, these graphical representations offer information on the molecule's size, structure, and possible reactive sites. Understanding molecular interactions and reactivity is aided by the ability to forecast potential interactions between molecules through the analysis of the charge distribution[3-4]. **Figure S11** presents the areas of negative and positive charge in the Sb-Fc (UNK0) complex being studied. In **Figure S11**, the molecular electrostatic potential (ESP) surface of the Sb-Fc (UNK0) ligand is shown, highlighting the spatial distribution of electrostatic charge throughout the molecular structure. The colour scale transitions from

blue, indicating positive electrostatic potential and electron-deficient areas, through green and yellow, representing neutral potential, to red, which signifies negative electrostatic potential and electron-rich areas. The red zones are primarily concentrated around the carbonyl oxygen, phenolic oxygen, and azomethine nitrogen atoms of the curcumin component, marking these as favourable sites for hydrogen bonding and nucleophilic interactions. Conversely, blue regions are mostly found over hydrogen atoms and parts of the indole and ferrocene units, suggesting potential sites for electrophilic interactions. The clear distinction between electron-rich and electron-deficient areas reveals a significant donor-acceptor electronic distribution, which supports intramolecular charge transfer within the conjugated system. This electrostatic polarization is anticipated to enhance ligand stabilization through groove binding and π–π stacking interactions with DNA base pairs. Overall, the ESP analysis confirms efficient charge separation and provides electrostatic evidence for the experimentally observed optical behaviour and binding capability of the Sb-Fc (UNK0) ligand.

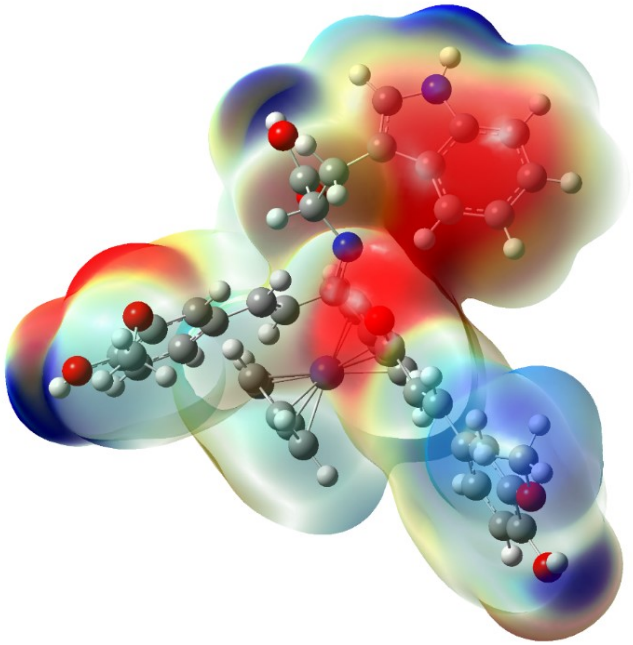

Figure S11: Molecular electrostatic potential (MEP) map of UNK0 ligand in the ground state using B3LYP/6-31G(d,p) and LANL2DZ level of theory.

Docking Analysis

1). 2LBY:

Estimated Free Energy of Binding = -5.96 kcal/mol [=(1)+(2)+(3)-(4)]

Estimated Inhibition Constant, Ki = 43.11 uM (micromolar) [Temperature = 298.15 K]

(1) Final Intermolecular Energy = -11.03 kcal/mol

vdW + Hbond + desolv Energy = -9.35 kcal/mol

Electrostatic Energy = -1.68 kcal/mol

(2) Final Total Internal Energy = -4.46 kcal/mol

(3) Torsional Free Energy = +5.07 kcal/mol

(4) Unbound System's Energy [=(2)] = -4.46 kcal/mol

2). 2HY9:

Estimated Free Energy of Binding = -5.72 kcal/mol [=(1)+(2)+(3)-(4)]

Estimated Inhibition Constant, Ki = 64.28 uM [Temperature = 298.15 K]

(1) Final Intermolecular Energy = -10.79 kcal/mol

vdW + Hbond + desolv Energy = -10.55 kcal/mol

Electrostatic Energy = -0.24 kcal/mol

(2) Final Total Internal Energy = -6.90 kcal/mol

(3) Torsional Free Energy = +5.07 kcal/mol

(4) Unbound System's Energy [=(2)] = -6.90 kcal/mol

3). 1BNA:

Estimated Free Energy of Binding = -5.06 kcal/mol [=(1)+(2)+(3)-(4)]

Estimated Inhibition Constant, Ki = 193.93 uM) [Temperature = 298.15 K]

(1) Final Intermolecular Energy = -10.14 kcal/mol

vdW + Hbond + desolv Energy = -11.23 kcal/mol

Electrostatic Energy = +1.09 kcal/mol

(2) Final Total Internal Energy = -6.21 kcal/mol

(3) Torsional Free Energy = +5.07 kcal/mol

(4) Unbound System's Energy [=(2)] = -6.21 kcal/mol

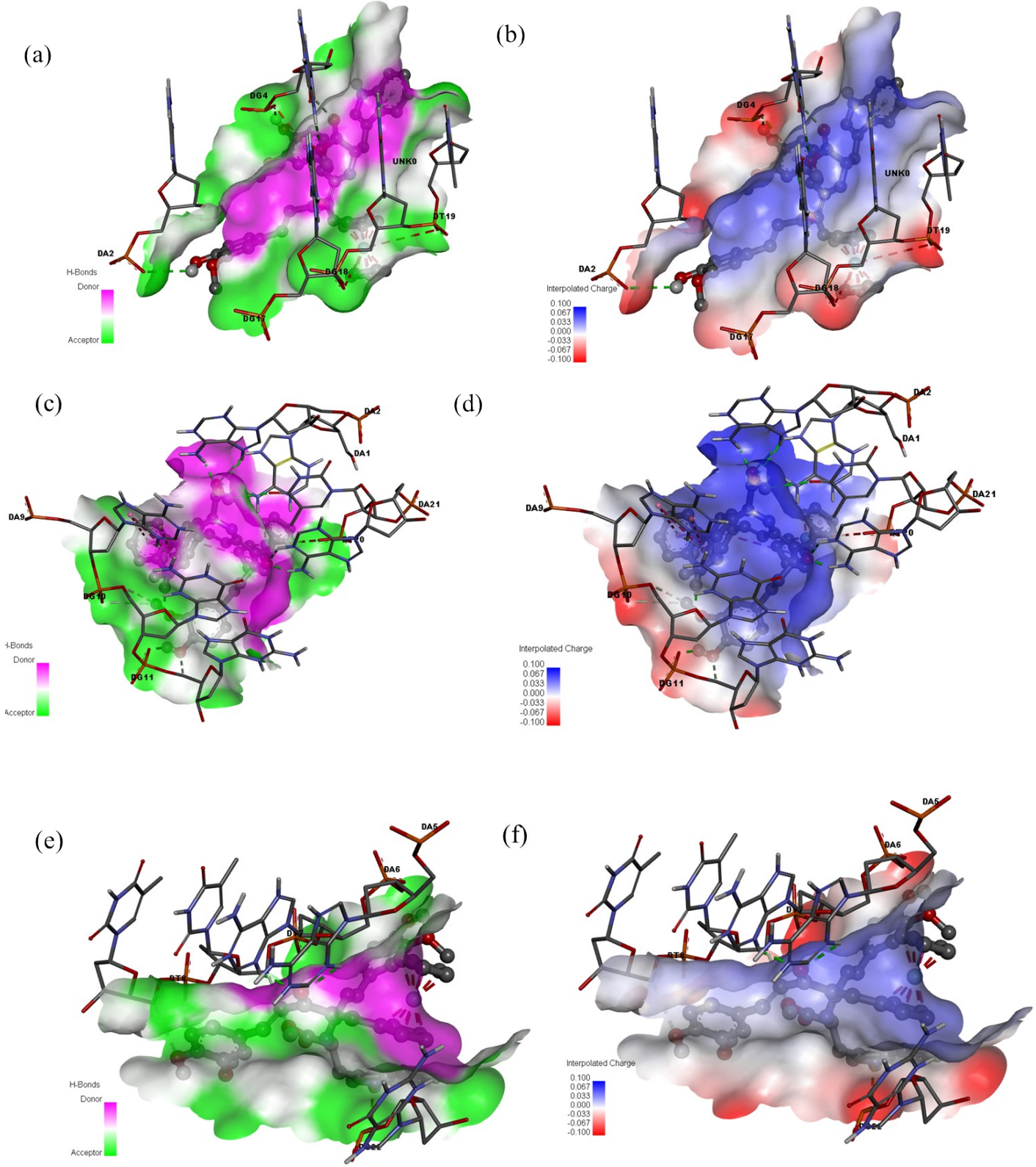

Figure S12: (a) H-bonds surface area of 2LBY with ligand Sb-Fc (UNK0), (b) interpolated charge surface area between ligand Sb-Fc (UNK0) and 2LBY. (c) H-bonds surface area of 2HY9 with ligand Sb-Fc (UNK0) , (d) interpolated charge surface area between ligand UNK0 and 2HY9. (e) H-bonds surface area of 1BDNA with ligand UNK0, and (f) interpolated charge surface area between ligand UNK0 and 1BDNA.

References

1. Prasad, O.; Sinha, L.; Misra, N.; Narayan, V.; Kumar, N.; Pathak, J., Molecular structure and vibrational study on 2, 3-dihydro-1H-indene and its derivative 1H-indene-1, 3 (2H)-dione by density functional theory calculations. *Journal of molecular structure: Theochem* **2010,** *940* (1-3), 82-86.
2. Fleming, I., Frontier orbitals and organic chemical reactions. *(No Title)* **1976**.
3. Mathammal, R.; Sangeetha, K.; Prasad, L. G.; Jayamani, V., Crystal growth, structural characterization and theoretical investigation on 3, 5-dinitrosalicylic acid monohydrate for nonlinear optical applications. *Spectrochimica Acta Part A: Molecular and Biomolecular Spectroscopy* **2015,** *144*, 200-214.
4. Scrocco, E.; Tomasi, J., Electronic molecular structure, reactivity, and intermolecular forces: an euristic interpretation by means of electrostatic molecular potentials. In *Advances in quantum chemistry*, Elsevier: 1978; Vol. 11, pp 115-193.